

cm^{-1} peak can be well accounted for without the need for symmetry-breaking mechanisms. Although the phonons originating from the LO branch at $k=0$ are strictly forbidden from first-order scattering in the present model, the large spatial extent of the nonzero $V_n(l\alpha)$'s has resulted in large contributions from A_{1g} projections of phonons arising from the LO branch away from $k=0$. Our results offer strong evidence that the diffuse nature of the higher-lying excited states and the consequent contribution to the scattering by the vibrations of a large number of ions play an important role in determining the evolution of the line shape of the one-phonon resonant Raman spectra of F centers in KCl as one tunes the incident photon energy through the optical absorption bands.

We are grateful to Dr. D. Pan for the use of unpublished experimental data (Fig. 1, 4765 Å), and to Professor F. Lüty and Professor H. Bilz, as well as to Dr. Pan, for numerous helpful discussions.

*Work partially supported by the National Science Foundation, Grant No. DMR75-10414 A01.

†Work partially supported by an Arizona State University graduate college fellowship.

‡Permanent address: Physics Department, Arizona State University, Tempe, Ariz. 85281.

¹D. S. Pan and F. Lüty, in *Light Scattering in Solids*, edited by M. Balkanski, R. C. C. Leite, and S. P. S. Porto (Flammarion, Paris, 1976), p. 539.

²D. B. Fitchen and C. J. Buchenauer, in *Physics of Impurity Centres in Crystals, Tallinn, U. S. S. R., 1970*, edited by G. S. Zavt (Academy of Science of Estonia S. S. R., Tallinn, U. S. S. R., 1972), p. 277.

³D. Robbins and J. B. Page, to be published.

⁴V. Hizhnyakov and I. Tehver, *Phys. Status Solidi* **21**, 755 (1967).

⁵R. T. Harley, J. B. Page, Jr., and C. T. Walker, *Phys. Rev. B* **3**, 1365 (1971).

⁶D. Y. Smith and G. Spinolo, *Phys. Rev.* **140**, A2121 (1965).

⁷B. S. Gourary and F. J. Adrian, *Phys. Rev.* **105**, 1180 (1957).

⁸U. Schröder, *Solid State Commun.* **4**, 347 (1966).

⁹F. Lüty, *Z. Phys.* **160**, 1 (1960).

¹⁰J. P. Buisson, M. Ghomi, and L. Taurel, *Solid State Commun.* **18**, 513 (1976).

Determination of Spatial Distribution of Charges in Thin Dielectrics

G. M. Sessler,* J. E. West, and D. A. Berkley
Bell Laboratories, Murray Hill, New Jersey 07994

and

G. Morgenstern
Technische Hochschule Darmstadt, Darmstadt, West Germany
(Received 8 December 1976)

We describe a high-resolution method to determine the spatial distribution of trapped charged or of a permanent dipole polarization in dielectrics. The method is capable of a resolution of $1 \mu\text{m}$ in a $25\text{-}\mu\text{m}$ -thick film.

Several techniques are available to measure the mean depth of charge distributions in a dielectric¹⁻⁴; however, it has only been possible to determine the actual charge distribution in thin films by heat-pulse-propagation experiments in a nonunique manner⁵ or by pressure-pulse experiments with a resolution of only about $100 \mu\text{m}$.⁶ In this Letter, we describe a technique capable of a resolution of about $1 \mu\text{m}$ in a $25\text{-}\mu\text{m}$ -thick film for determining the spatial distribution of trapped charges or of a permanent dipole polarization in dielectrics.

The present method depends on measurements of the charges released from an electrode on one side of a two-sided metallized dielectric while a

virtual electrode generated by a particle beam is swept through the sample. The basic setup for the experiment is shown in Fig. 1. The particle beam, assumed to be a monoenergetic electron beam in the present case, is incident through the front electrode under short-circuit conditions (front and rear electrodes connected by a low-impedance measuring setup). It generates a radiation-induced conductivity³ to a depth determined by the maximum electron penetration which corresponds approximately to the c.s.d.a. (continuous slowing-down approximation) range. Thus a virtual electrode is created at the plane of maximum penetration. Since the electron range depends on particle energy, the virtual electrode

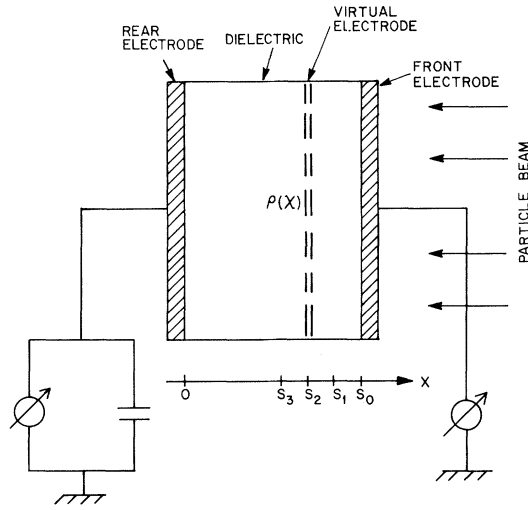


FIG. 1. Schematic diagram of the setup for measurement of the charge distribution in a dielectric.

can be swept through the dielectric by increasing the energy of the electrons.

It is assumed that the dielectric carries a volume-charge distribution $\rho(x)$ characterized by

$$\rho(x) = \rho_r(x) + \rho_p(x), \quad (1)$$

where $\rho_r(x)$ is the volume density of the real charges while

$$\rho_p(x) = -dP_p/dx \quad (2)$$

represents the contribution of the permanent dipole polarization P_p . Under short-circuit conditions an induction charge per unit area

$$q = -s^{-1} \int_0^s (s-x)\rho(x) dx \quad (3)$$

resides on the rear electrode, where $x=s$ marks the location of the virtual electrode.

Differentiating qs from Eq. (3) twice with respect to s yields, according to Leibniz's theorem,⁷

$$\int_0^s \rho(x) dx = -d(qs)/ds, \quad (4)$$

$$\rho(s) = -d^2(qs)/ds^2.$$

The charge density at any location in the dielectric can thus be found by sweeping the virtual electrode through the dielectric and determining the second derivative of qs with respect to s .

If the virtual electrode is moved through the dielectric in equidistant steps Δs rather than continuously, the differential in Eq. (4) can be replaced by a difference quotient. Assuming that the electrode locations are s_1, s_2, \dots, s_n and that the corresponding electrode charge densities are

given by q_1, q_2, \dots, q_n one has from Eq. (4) the approximation

$$\rho(s_n) \approx -(\Delta s)^{-2} [q_{n-1}s_{n-1} - 2q_n s_n + q_{n+1}s_{n+1}], \quad (5)$$

where $s_{n-k} = s_n + k\Delta s$. Substitution into Eq. (5) yields, with $\Delta q_n = q_{n-1} - q_n$,

$$\Delta s \rho(s_n) \approx - (s_{n+1}/\Delta s)(\Delta q_n - \Delta q_{n+1}) - 2\Delta q_n. \quad (6)$$

The charge density $\rho(s_n)$ at $x = s_n$ may thus be determined by measuring the electrode charges Δq_n and Δq_{n+1} released upon moving the virtual electrode from $x = s_{n-1}$ to s_n and from $x = s_n$ to s_{n+1} , respectively.

Without further measures, the method does depend on a complete transfer of the virtual electrode from $x = s_{n-1}$ to $x = s_n$. This means that the entire original charge within $s_n \leq x \leq s_{n-1}$ as well as the charge supplied by the beam has to leave the dielectric or be otherwise compensated, and that an induction charge

$$q_i = -s^{-1} \int_0^{s_n} x \rho(x) dx,$$

corresponding to the original charge still residing in the volume $0 \leq x \leq s_n$, is deposited at the virtual electrode. Such a complete transfer cannot be expected in general^{3,8} for dielectrics described here. [See Eq. (8), Ref. 3.]

This problem can be solved by utilizing a calibration run with an initially uncharged sample. The calibration consists of the irradiation of the virgin sample with the same beam energies under the same conditions. To make the calibration run and the actual run comparable, the irradiation at each energy has to be maintained for a time period long enough so that the fields in the irradiated part of the two samples are exactly identical. This is possible⁹ by maintaining the irradiation for a time period of $t_0 \gg \bar{\tau} = \epsilon s_0 / g s_n$,³ where ϵ is the dielectric constant and g is the prompt conductivity. The virtual electrode is then located⁹ at the plane $x = s_n$ where the local time constant $\tau(s_n) = \epsilon / g(s_n)$ equals t_0 .

The above concept of determining charge distribution was applied to previously charged polyfluoroethylenepropylene (FEP) samples. The experiments were performed with a scanning-electron microscope providing a monoenergetic, diffuse beam whose energy can be adjusted in the range 5 to 55 keV. As indicated in Fig. 1, the front electrode of the sample was connected to an electrometer to monitor the irradiation current while the rear electrode was connected to a high-capacitance charge-measuring setup to determine the Δq values needed to calculate $\rho(x)$ with Eq. (6).

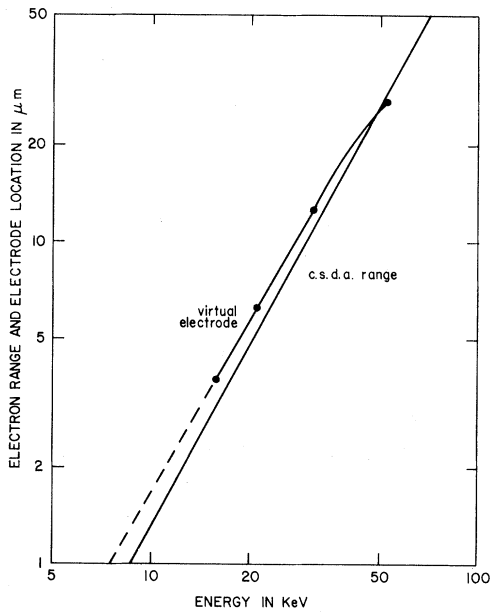


FIG. 2. Electron range (c.s.d.a. range) and location of virtual electrode (equivalent to 1% transmission range) in FEP.

The sample was irradiated in steps with electrons having energies between 7.6 and 30 keV. Current densities between 2.3 and 7.4×10^{-10} A/cm², adjusted for constant $g(s_n)$, and intermission periods of 5 min were used for the virgin and charged samples.

For the above parameters, the location of the virtual electrode corresponds⁹ to a transmission coefficient of the primary electrons of approximately 10^{-2} . The electrode location was thus found by measuring the energy for which 1% transmission was obtained on samples of different thickness. The location of the virtual electrode so determined is compared in Fig. 2 with the c.s.d.a. range.¹⁰ For the above initial energy, a step size of $1 \mu\text{m}$ is obtained.

The charge distribution in a $25\text{-}\mu\text{m}$ FEP sample originally metallized on its rear side, charged by injection of a 20-keV electron beam, annealed for 1 h at 100°C , thereafter metallized on its front side, and then subjected to the charge distribution measurements, is shown in Fig. 3. The distribution has maxima at depths of 1 and $5 \mu\text{m}$ from the front surface. During the original charging of this sample, a virtual electrode at a depth of $5 \mu\text{m}$ was formed (see Fig. 2) and the charge is expected to accumulate there because of the prevailing field direction in the one-sided metallized sample. The maximum at $1 \mu\text{m}$ is

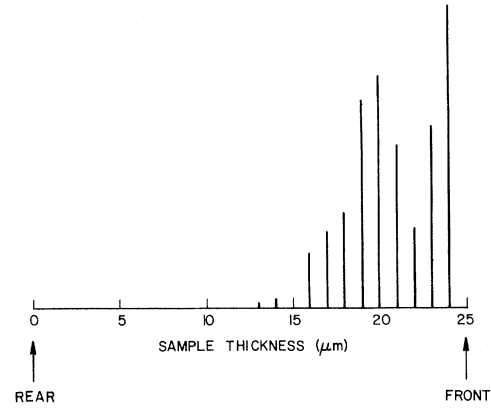


FIG. 3. Charge distribution in a $25\text{-}\mu\text{m}$ FEP film, charged by injection of a 20-keV electron beam through its front surface and annealed for 1 h at 100°C prior to measurement.

probably due to the (weak) field in the front part of the foil caused by secondary emission during charging, as observed by Collins.⁵ Since the resulting positive charges stay on the surface, a negative depletion layer forms close to the surface. Upon metallization, the positive surface charges disappear while the depletion layer remains. The relative charge content of this layer (about 30% of the total) corresponds to the relative amount of positive charge found by Collins.⁵

The method is destructive in the sense that a sample is discharged after the interrogation. This is, however, no serious limitation since most electrets can be formed reproducibly in any desired number of species or can be made large enough to allow measurements over a small section of their area.

The method described in this paper is the first procedure capable of providing unique information about charge distributions in dielectrics with a resolution of the order of $1 \mu\text{m}$. It is therefore capable of detecting a wealth of data about thin-film electrets previously not amenable to experimental studies. It can similarly be used to investigate charge distributions in metal oxides, photoconductors, or other materials which could previously only be investigated with respect to charge-centroid location. This is particularly important in view of the great current interest in charge distributions and charge dynamics in such materials.¹¹⁻¹³

The authors are grateful to Professor B. Gross and Professor M. M. Perlman for helpful suggestions and to Mr. R. Kubli for technical assistance.

*Now at the Technische Hochschule Darmstadt, Darmstadt, West Germany.

¹G. M. Sessler and J. E. West, in *Annual Report Conference on Electrical Insulation and Dielectric Phenomena* (National Academy of Science, Washington, D. C., 1971), pp. 8-16; G. M. Sessler, *J. Appl. Phys.* **43**, 408 (1972).

²B. Gross, J. Dow, and S. V. Nablo, *J. Appl. Phys.* **44**, 2459 (1973).

³B. Gross, G. M. Sessler, and J. E. West, *J. Appl. Phys.* **45**, 2841 (1975).

⁴R. E. Collins, *Appl. Phys. Lett.* **26**, 675 (1975).

⁵R. E. Collins, to be published.

⁶P. Laurenceau, G. Dreyfus, and J. Lewiner, to be published.

⁷I. S. Sokolnikoff and R. M. Redheffer, *Mathematics of Physics and Modern Engineering* (McGraw-Hill, New York, 1958), p. 262.

⁸J. F. Fowler, *Proc. Roy. Soc. London, Ser. A* **236**, 464 (1956).

⁹G. M. Sessler, J. E. West, and D. A. Berkley, to be published.

¹⁰L. Pages, E. Bertel, H. Joffre, and L. Shlavenitis, *At. Data* **4**, 1 (1972).

¹¹T. J. Sonnonstine and M. M. Perlman, *Phys. Rev. B* **12**, 4434 (1975).

¹²P. C. Arnett and B. H. Yun, *Appl. Phys. Lett.* **26**, 94 (1975).

¹³H. Scher and E. W. Montroll, *Phys. Rev. B* **12**, 2455 (1975).

Soft Modes and the Structure of the DNA Double Helix*

James M. Eyster and E. W. Prohofsky

Physics Department, Purdue University, West Lafayette, Indiana 47907

(Received 29 July 1976)

We show that a soft mode arises when the vibrational modes of double-helical DNA are perturbed by increasing the electrostatic or Van der Waals interactions between atoms. We believe this soft mode drives the *B* to *A* conformation change which is observed when DNA has water of hydration removed from it.

We have applied the method of vibrational mode softening to investigate conformation changes (i.e., changes in three-dimensional structure) in double-helical DNA. Conformation changes of these macromolecules are analogous to displacive phase changes in crystalline solids. We have calculated a mode softening which would drive the double helix from its *B* conformation to its *A* conformation. The mode is not softened by temperature change, but rather by changes in the macromolecular environment which mimics the conditions which cause the conformation change experimentally.

The DNA double helix can take on several conformations.¹ When dissolved in water or in gels at high humidity (much water of hydration) it is found in the *B* conformation. Upon drying the gel in an atmosphere of less than 92% relative humidity, it converts to the *A* conformation. RNA on the other hand is found only in *A*-type conformations. It has been suggested that DNA switches to *A* conformation locally when transcribing RNA *in vivo* and that this conformation change is an important switching mechanism in the biological function of nucleic acid.²

We have carried on extensive theoretical investigations of the lattice dynamics of DNA and RNA helices.³ These calculations were made using valence and Urey-Bradley force fields which were

obtained, by various authors, by refinement from the observed spectra of the constituent parts of nucleic acid. The calculations were done for artificial homopolymer DNA in which all the base units in a single helix were the same. Two such double-helical DNA compounds exist—poly(dA)·poly(dT) and poly(dG)·poly(dC)—where the bases are adenine, thymine, guanine, and cytosine, respectively. These homopolymer duplexes are available and a considerable amount of experimental ir and Raman analysis has been done for all the occurring conformations. A comparison of our theoretical lines with those observed shows quite good agreement for those regions of the spectrum where data exist.³ In our calculations for both poly(dG)·poly(dC) and poly(dA)·poly(dT) the lowest-lying optical mode is one in which the two single helices move up and down relative to each other along the double-helix axis. It is this mode which softens in our calculations.

The eigenvector of the mode that softens agrees very well with the description of the *B* to *A* conformation change. The *B* conformation has the bases of the helix perpendicular to the helix axes. In the *A* conformation, the bases are tilted from the perpendicular. The soft mode in which the two helices displace relative to each other along the axis does lead to such a tilting of the bases.

In doing our calculations for the soft mode, we